Available online at www.sciencedirect.com

ScienceDirect

Procedia Engineering 199 (2017) 1798–1803

Procedia Engineering

www.elsevier.com/locate/procedia

X International Conference on Structural Dynamics, EURODYN 2017

Hysteresis based vibration control of base-isolated structures

José Rodellar[a], Guillem Garcia[a], Yolanda Vidal[a], Leonardo Acho[a], Francesc Pozo[a,*]

[a]*Control, Dynamics and Applications (CoDAlab), Departament de Matemàtiques, Escola d'Enginyeria de Barcelona Est (EEBE), Universitat Politècnica de Catalunya (UPC), Campus Diagonal-Besòs (CDB), Eduard Maristany, 6–12, Sant Adrià de Besòs (Barcelona) 08930, Spain*

Abstract

An active control strategy for base-isolated structures is proposed in this work. The key idea comes from the observation that passive base isolation systems are hysteretic. Thus, an hysteresis based vibration control is designed in a way that the control force is smooth and limited by a prescribed bound. A model of a three-story building is used to study and compare the efficacy of a passive pure friction damper alone, with the addition of the proposed active control. We introduce a rate limiter to the actuator to simulate its limited speed capacity, present in every physical actuator. Simulations demonstrate that our active control strategy significantly reduces base displacements and shears without an increase in drift or accelerations.

Peer-review under responsibility of the organizing committee of EURODYN 2017.

Keywords: hysteresis, base-isolated building, active control, rate limiter

1. Introduction

Civil structures are affected by several kinds of dynamic excitations such as earthquakes, winds or traffic loading. In this regard, base isolation has been extensively considered as an adequate technology to protect flexible building structures producing a dynamic decoupling of the structure from its foundation [1]. However, the resulting base displacement may be excessive. Consequently, the combination of active or semi-active systems installed along with base-isolation bearings may alleviate the negative effects of such loads. In this work, we propose a hybrid control system where the active control force is supplied by an appropriate actuator taking care of the saturation problem and rate limits. Every physical actuator is prone to saturations because of its limited capacities in amplitude and speed. Actuator amplitude limitation or rate limitation constitutes an important constraint on linear and nonlinear control design. Generally, actuator saturations are protection systems whose main objective is to avoid operating an actuator with violent control actions (that can be produced by a failure or a low quality of the control law implemented), and also avoid damaging the actuator and/or the structure (or object) it manipulates [2]. Controllers that ignore actuator limitations may cause the closed loop system performance to degenerate or even make the closed loop system unstable, and decrease the actuators lifetime.

The main contribution of this work comes from the observation that passive base isolation systems are hysteretic [3]. It is well known that these systems are dissipative, and their energy dissipation comes from the hysteresis effect

* Corresponding author. Tel.: +34-934-137-316 ; fax: +34-934-137-401.
E-mail address: francesc.pozo@upc.edu

1877-7058
Peer-review under responsibility of the organizing committee of EURODYN 2017.
10.1016/j.proeng.2017.09.090

of these devices [3]. But being passive, they lack the benefits of active control. The contribution of this work is precisely to take advantage of an hysteretic energy dissipator but increasing its efficiency with its active realization. The controller is designed in such a way that: (i) the force that is applied to the structure is bounded by a prescribed quantity –so that preventing the actuator to saturate–; and (ii) the rate-of-change of the active control force is also limited, thus providing an smooth control action.

The saturation limit is a priori limited by the controller design. As a consequence, the saturation can be neglected for any consideration and analysis. However, the rate limiter needs to be taken into account instead.

Experimental results demonstrate the ability of the design method to attenuate the effects of seismic excitation and simultaneously avoid the adverse effects of actuator rate limiter saturation.

2. Control design

2.1. System description

Consider a hysteretic base-isolated building structure as shown in Figure 1. The equation of motion of a seismically excited structure with multiple degrees of freedom that is controlled by a single active force acting on the first floor can be described as follows:

$$\mathbf{M}\ddot{\mathbf{x}} + \mathbf{C}\dot{\mathbf{x}} + \mathbf{K}\mathbf{x} = -\mathbf{M}\boldsymbol{\Lambda}\ddot{x}_g - \boldsymbol{\Gamma} f + \boldsymbol{\Gamma} u, \tag{1}$$

where $\ddot{x}_g$ is the absolute ground acceleration, $\mathbf{x} = [x_1, x_2, \ldots, x_n]^T \in \mathbb{R}^n$ represents the horizontal displacement of each floor with respect to the ground, n is the number of floors, $\dot{\mathbf{x}}$ and $\ddot{\mathbf{x}}$ are the n dimensional vectors of the velocities and accelerations of the floors of the structure, $\mathbf{M}, \mathbf{C}$ and $\mathbf{K}$ are $n \times n$ mass, damping and stiffness matrices, respectively, and have the following form:

$$\mathbf{M} = \begin{bmatrix} m_1 & 0 & \cdots & 0 \\ 0 & m_2 & \ldots & 0 \\ \vdots & \vdots & \ddots & \vdots \\ 0 & 0 & \ldots & m_n \end{bmatrix}, \ \mathbf{C} = \begin{bmatrix} c_1 + c_2 & -c_2 & \cdots & 0 & 0 \\ -c_2 & c_2 + c_3 & \ldots & 0 & 0 \\ \vdots & \vdots & \ddots & \vdots & \vdots \\ 0 & 0 & \ldots & c_{n-1} + c_n & -c_n \\ 0 & 0 & \ldots & -c_n & c_n \end{bmatrix}, \ \mathbf{K} = \begin{bmatrix} k_1 + k_2 & -k_2 & \cdots & 0 & 0 \\ -k_2 & k_2 + k_3 & \ldots & 0 & 0 \\ \vdots & \vdots & \ddots & \vdots & \vdots \\ 0 & 0 & \ldots & k_{n-1} + k_n & -k_n \\ 0 & 0 & \ldots & -k_n & k_n \end{bmatrix}.$$

The base isolation is described as a single degree of freedom with horizontal displacement x_1. It is assumed to exhibit a linear behavior characterized by mass, damping and stiffness m_1, c_1 and k_1, respectively, plus a nonlinear behavior represented by a hysteretic restoring force f, which can be represented by the Bouc–Wen model [4] in the following form:

$$f = c_0 \dot{x}_1 + \alpha z \tag{2}$$

$$\dot{z} = -\gamma |\dot{x}_1| z |z|^{\nu-1} - \beta \dot{x}_1 |z|^{\nu} + A \dot{x}_1 \tag{3}$$

where z is the evolutionary variable that provides information on the history dependence of the response and the parameters γ, β, ν and A govern the linearity and smoothness of the transition from elastic to plastic response and c_0 and α are base-isolator related parameters defined as in [5]. Finally, u is the control force supplied by an appropriate actuator, $\boldsymbol{\Lambda}$ is the influence coefficient matrix of size $n \times 1$ and $\boldsymbol{\Gamma}$ is the vector of size n that specifies the placement of the base-isolator and the active control force. $\boldsymbol{\Lambda}$ and $\boldsymbol{\Gamma}$ are defined as follows:

$$\boldsymbol{\Lambda} = \begin{bmatrix} 1 & 0 & \cdots & 0 \end{bmatrix}^T \in \mathbb{R}^n, \ \boldsymbol{\Gamma} = \begin{bmatrix} 1 & 1 & \cdots & 1 \end{bmatrix}^T \in \mathbb{R}^n. \tag{4}$$

2.2. Hysteretic control

2.2.1. Control objective and design

We seek for an active control strategy showing the following features: (i) to be a *bounded* active control in the sense that the control force that is applied to the structure is limited by a prescribed magnitude; (ii) to be a *smooth* controller

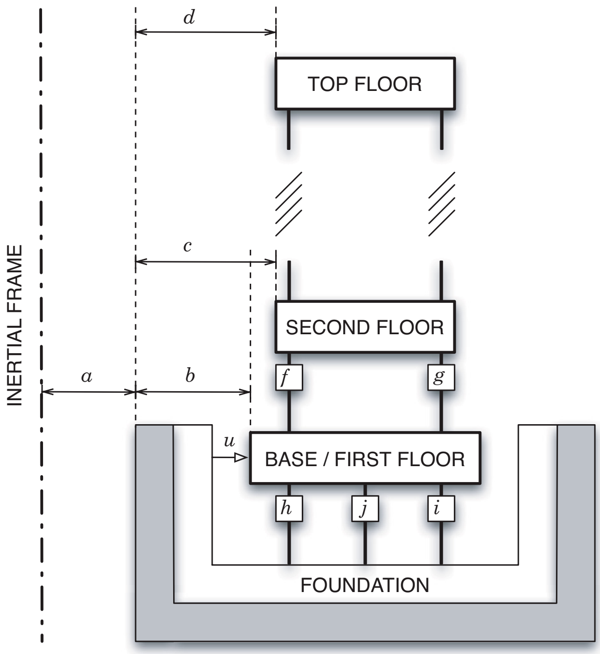

Fig. 1. Base-isolated structure with an active control.

in the sense that the *rate-of-change* of the control force is restricted; (iii) to be an active control using only local *velocity* information between the points where the device supplying the active force is connected; (iv) to guarantee the boundedness of all the trajectories of the closed-loop system when the ground motion is striking the building; and (v) to be an *admissible* controller in the sense that when the ground motion is not present, the closed-loop system is asymptotically stable.

To this end, we propose an active control strategy with the following structure:

$$u = -\rho \cdot g(\dot{x}_1) \tag{5}$$

where the coefficient ρ is a positive real number and $\dot{x}_1$ the relative velocity of the base of the structure with respect to the ground. On one hand, when $g(\dot{x}_1) = \dot{x}_1$, the controller is equivalent to the classical proportional velocity control equivalent to a linear damper. On the other hand, when $g(\dot{x}_1)$ is the signum function of the velocity, that is, $g(\dot{x}_1) = \operatorname{sgn}(\dot{x}_1)$, the controller is equivalent to a pure friction damper. This strategy has already been reported in the literature. For instance, the control strategy in equation (5) when $g(\dot{x}_1) = \operatorname{sgn}(\dot{x}_1)$ is satisfactorily applied to a benchmark base-isolated building both as an active control [1,6] or as a semi-active control strategy [7]. A different function is considered in [8,9], where $g(\dot{x}_1)$ is defined as the product of two hyperbolic functions in the following form:

$$g(\dot{x}_1) = \operatorname{sech}\left(\frac{\dot{x}_1}{\omega}\right) \cdot \tanh\left(\frac{\dot{x}_1}{\omega}\right), \tag{6}$$

where ω is a positive design parameter. In the first case [8], the active control is applied to the same benchmark structure as in [1] but a semi-active control implementation is also introduced. In the second case [9], the active control is applied to a benchmark highway bridge proposed by the American Society of Civil Engineering (ASCE) Committee on structural control [5]. An interesting characteristic of the reported functions $g(\dot{x}_1) = \dot{x}_1$, $g(\dot{x}_1) = \operatorname{sgn}(\dot{x}_1)$ and the function in equation (6) is that all of them are passive in the sense that $g(\dot{x}_1) \cdot \dot{x}_1 \geq 0$, $g(0) = 0$.

In this work, a different function g is proposed that is based on an evolutionary variable η as follows:

$$g(\dot{x}_1) = \eta \tag{7}$$

$$\dot{\eta} = \varphi \left\{ -\eta + b \operatorname{sgn}\left[c\dot{x}_1 + a \operatorname{sgn}(\eta) \right] \right\} \tag{8}$$

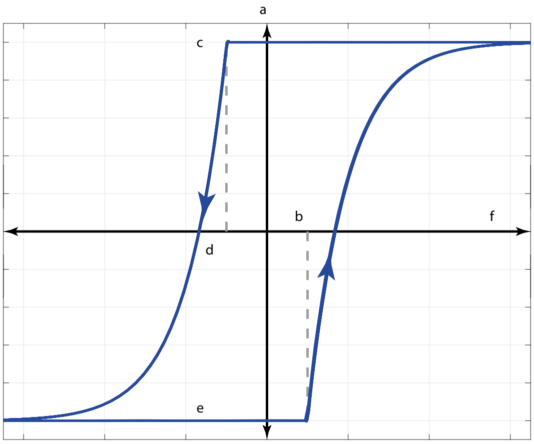

Fig. 2. Hysteretic behavior of the system described in equation (8).

where φ is a positive real number and a, b and c –also positive– are the hysteresis loop parameters shown in Figure 2. It is worth noting that this is a bounded-input bounded-output (BIBO) stable system based on the hysteretic system previously proposed in [10]. In the current approach, the system proposed in [10] is modified by adding c, a third hysteresis loop parameter that multiplies the velocity. The transition speed between b and $-b$ or viceversa is controlled by the positive parameter φ while b is an upper bound on the magnitude of $\eta(t)$, that is, $|\eta(t)| \leq b,\ t \geq 0$. Consider two models (7)-(8) whose parameters are such that $\varphi_1 = \varphi_2,\ a_2 = \kappa a_1,\ b_2 = b_1,\ c_2 = \kappa c_1$, where κ is a positive constant, and with the initial conditions $\eta_2(0) = \eta_1(0) = 0$. Then, and for any input $\dot{x}_1(t)$, both models deliver the same output u_h, which means that the model in equations (7)-(8) is overparameterized.

The following assumption is specified for the system in equations (1)-(3):

Assumption 1. *The ground acceleration* $\ddot{x}_g$ *in equation* (1) *is unknown but bounded. That is, there exists a known constant* G *such that* $\left|\ddot{x}_g(t)\right| \leq G,\ t \geq 0$.

Additionally, Theorem 1 in [11] guarantees the existence of an upper bound Z on the evolutionary variable $z(t)$ in equation (3), that is, $|z(t)| \leq Z,\ t \geq 0$. This upper bound, G, is computable and independent of the boundedness of the base displacement $x_1(t)$ or velocity $\dot{x}_1(t)$.

The next theorem states the main contribution of this work with respect to the control design.

Theorem 1. *Consider the nonlinear system in equations* (1)-(3) *subject to Assumption 1. Then, the control objective is achieved by the following control law:*

$$u_h = -\rho_h \eta, \tag{9}$$

$$\dot{\eta} = \varphi \left\{-\eta + b\,\mathrm{sgn}\left[c\dot{x}_1 + a\,\mathrm{sgn}\,(\eta)\right]\right\}, \tag{10}$$

where a, b, c, φ *and* ρ_h *are positive design parameters.*

Proof. Similarly as in [8], the proof is based on the boundedness of the ground acceleration, the evolutionary variable z in equation (3) and the control law u_h in equations (9)-(10). We have omitted the details of the proof for space reasons. □

3. Simulation results

For assessing the performance of the proposed active control scheme, a base-isolated three-storey benchmark building structure described by the authors of [12] is considered. This model has been intensively utilized by many researchers at the structural dynamics and control fields. For instance, this benchmark has been recently used in two semi-active control applications by Alqado et al. [13,14].

For this setup, the mass, stiffness and damping matrices are given as follows [12]:

$$\mathbf{M} = \begin{bmatrix} 98.3 & 0 & 0 \\ 0 & 98.3 & 0 \\ 0 & 0 & 98.3 \end{bmatrix} [\![\mathrm{kg}]\!],\ \mathbf{C} = \begin{bmatrix} 175 & -50 & 0 \\ -50 & 100 & -50 \\ 0 & -50 & 50 \end{bmatrix} \times 10^5\ [\![\mathrm{Ns/m}]\!],\ \mathbf{K} = \begin{bmatrix} 12.0 & -6.84 & 0 \\ -6.84 & 13.68 & -6.84 \\ 0 & -6.84 & 6.84 \end{bmatrix} \times 10^5\ [\![\mathrm{N/m}]\!] \quad (11)$$

while the Bouc–Wen parameters in equations (2)-(3) that models the base-isolator are given in Table 1.

Table 1. Bouc–Wen parameters in equations (2)-(3) of the base-isolator [13].

Parameter	Value	Parameter	Value
c_0	2.1×10^3 [[Ns/m]]	α	1.4×10^4 [[N/m]]
γ	3.63×10^6 [[m^{-2}]]	β	3.63×10^6 [[m^{-2}]]
A	301	ν	2

Five different ground acceleration time history records are used to excite the model of the structure. These records include Newhall, Sylmar, El Centro, Rinaldi, and Kobe. The simulation results of the hysteretic control in equations (9)-(10) are compiled in Table 2 for the fault parallel (FP) component of these records. The results of the proposed control u_h are also compared with the pure friction damper in [1,6], defined as $u_s = -\rho_s \operatorname{sgn}(\dot{x}_1)$, and with an actuator rate limiter of 65000 N/S.

The evaluation is described in terms of the evaluation criteria defined in [5]. The five ground acceleration time history records are used at the full intensity for the computation of the evaluation criteria. Evaluation criteria smaller than 1 indicate that the response of the uncontrolled structure is bigger than that of the controlled structure. Contrarily, evaluation criteria larger than 1 indicate that the controlled response of the structure is bigger than that of the uncontrolled case. Evaluation criteria larger than 1 in Table 2 are highlighted with a grey colored cell background.

3.1. Simulation results

The base and structural shears are reduced between 4 and 37% in a majority of earthquakes (except Sylmar, and Kobe). The reduction in base displacement is between 14 and 65% in all cases except Kobe. Reductions in the interstorey drifts between 1 and 25% are achieved in all earthquakes but Kobe when compared with the uncontrolled case. The floor accelerations are also reduced –by up to 35%– in a majority of earthquakes (except Sylmar, and Kobe).

From a general point of view, the benefit of the active control strategy is the reduction in base displacement (J_3) and shear (J_1, J_2) of up to 40% without and increase in drift (J_4) or acceleration (J_5). The reduction in the peak base displacement J_3 if the base-isolated structure is one of the most important criteria during strong earthquakes.

Although both the peak base displacement (J_3) and the peak absolute floor acceleration (J_5) are significantly reduced in a majority of earthquakes, it is worth noting that their equivalent root mean square (RMS) measures (J_7 and J_8, respectively) are remarkably reduced in all the earthquakes. For instance, the reduction in RMS base displacement is between 39 and 90% and the reduction in RMS absolute floor acceleration fluctuate between 17 and 82%. This means that even in a case where the peak base displacement in the controlled structure is increased by 0.3% (fault normal component of Kobe, not shown in Table 2)–with respect to the uncontrolled case– the RMS base displacement is reduced by 41%. Similarly, when the fault parallel component of Kobe earthquake is used to excite the structure, the peak absolute floor acceleration is increased by 9.7% while the equivalent RMS measure is reduced by 52.1%. These two RMS-related evaluation criteria are somehow linked with the oscillating behavior of the structure. Therefore, low RMS-related performance indices imply a reduction in the overall structural charges that affect the building. The bound on the control force is defined as the product of the design parameters ρ_h and b in equations (9) and (10). Consequently, the performance index J_6 –which is a measure of the relative control effort of the proposed strategy– lie within a range of acceptable values (45 – 70%).

4. Concluding remarks

A comparison study, covering fully active and pure friction damper, is performed. The response to several earthquake excitations is computed. Numerical simulations suggest that the proposed active control shows significant

Table 2. Results of the controllers' evaluation criteria for a limited rate of 65000 N/S (FP-x and FN-y)

Earthquake	Case	J_1	J_2	J_3	J_4	J_5	J_6	J_7	J_8
Newhall	u_s	0.6785	0.7583	0.5803	0.8388	0.9663	0.8357	0.4965	0.6043
	u_h	0.8621	0.8647	0.5421	0.8654	0.9112	0.7020	0.3440	0.6726
Sylmar	u_s	0.9341	0.9359	0.5921	0.8976	1.0276	0.6767	0.5018	0.6829
	u_h	1.0652	1.0238	0.5758	0.9232	1.1672	0.6375	0.3763	0.6938
El Centro	u_s	0.7486	0.8505	0.2797	0.9666	1.0078	0.8855	0.3136	1.1954
	u_h	0.9091	0.8971	0.5762	0.8810	0.9641	0.5851	0.1847	0.7533
Rinaldi	u_s	0.5678	0.5760	0.5392	0.7811	0.6051	0.7706	0.3864	0.5004
	u_h	0.8309	0.7243	0.5018	0.8359	0.7691	0.5841	0.3264	0.5910
Kobe	u_s	0.4851	0.5529	0.5901	0.8403	0.6159	1.6206	0.4894	0.6363
	u_h	1.0444	1.0479	0.8679	1.0018	1.0966	0.4502	0.3488	0.4792

promise in base isolation applications, even taking into account the rate limit of the used actuator. In particular, both the peak base displacements and the peak absolute floor accelerations are significantly reduced in a majority of earthquakes, and their equivalent RMS measures are remarkably reduced in all the studied earthquakes. Finally, the control action is limited by a prescribed magnitude.

Acknowledgements

This work has been partially funded by the Spanish Ministry of Economy and Competitiveness through the research projects DPI2014-58427-C2-1-R and DPI2015-64170- R, and by the Catalonia Government (Generalitat de Catalunya) through the research project 2014 SGR 859.

References

[1] F. Pozo, P. M. Montserrat, J. Rodellar, L. Acho, Robust active control of hysteretic base-isolated structures: Application to the benchmark smart base-isolated building, Structural Control and Health Monitoring 15 (2008) 720–736.

[2] R. Yuan, X. Tan, G. Fan, J. Yi, Robust adaptive neural network control for a class of uncertain nonlinear systems with actuator amplitude and rate saturations, Neurocomputing 125 (2014) 72–80.

[3] D. Cancellara, F. De Angelis, A base isolation system for structures subject to extreme seismic events characterized by anomalous values of intensity and frequency content, Composite Structures 157 (2016) 285–302.

[4] F. Ikhouane, J. Rodellar, Systems with hysteresis: analysis, identification and control using the Bouc-Wen model, John Wiley & Sons, 2007.

[5] P. Tan, A. K. Agrawal, Benchmark structural control problem for a seismically excited highway bridge – Part II: phase I sample control designs, Structural Control and Health Monitoring 16 (2009) 530–548.

[6] G. Pujol, L. Acho, F. Pozo, A. Rodríguez, Y. Vidal, A velocity based active vibration control of hysteretic systems, Mechanical Systems and Signal Processing 25 (2011) 465–474.

[7] A. Bahar, F. Pozo, L. Acho, J. Rodellar, A. Barbat, Hierarchical semi-active control of base-isolated structures using a new inverse model of magnetorheological dampers, Computers & structures 88 (2010) 483–496.

[8] F. Pozo, L. Acho, J. Rodellar, Hyperbolic control for vibration mitigation of a base-isolated benchmark structure, Structural Control and Health Monitoring 16 (2009) 766–783.

[9] G. Pujol, L. Acho, F. Pozo, J. Rodellar, A nonlinear damping control for the vibration mitigation of the benchmark highway bridge, Structural Control and Health Monitoring 16 (2009) 586–598.

[10] C. Tutivén, Y. Vidal, L. Acho, J. Rodellar, Hysteresis-based design of dynamic reference trajectories to avoid saturation in controlled wind turbines, Asian Journal of Control (2016).

[11] F. Ikhouane, V. Mañosa, J. Rodellar, Adaptive control of a hysteretic structural system, Automatica 41 (2005) 225–231.

[12] S. J. Dyke, Acceleration feedback control strategies for active and semi-active control systems: modeling, algorithm development, and experimental verification, Ph.D. thesis, directed by B. F. Spence, Jr. for the Department of Civil Engineering and Geological Sciences.University of Notre Dame, 1996.

[13] T. E. Alqado, G. Nikolakopoulos, Posicast control of structures using mr dampers, Structural Control and Health Monitoring (2016).

[14] T. E. Alqado, G. Nikolakopoulos, L. Dritsas, Semi-active control of flexible structures using closed-loop input shaping techniques, Structural Control and Health Monitoring (2016).